

*Just Accepted by Free Radical Research*

## Astaxanthin diferulate as a bifunctional antioxidant

Thiago Bueno Ruiz Papa, Vagner Dantas Pinho, Eduardo Sanches Pereira do Nascimento, Willy Glen Santos, Antonio Carlos Bender Burtoloso, Leif Horsfelt Skibsted, and Daniel Rodrigues Cardoso

doi: 10.3109/10715762.2014.982112

### Abstract

Astaxanthin when esterified with ferulic acid is better singlet-oxygen quencher with  $k_2 = (1.58 \pm 0.1) 10^{10} \text{ L mol}^{-1}\text{s}^{-1}$  in ethanol at 25°C compared to astaxanthin with  $k_2 = (1.12 \pm 0.01) 10^9 \text{ L mol}^{-1}\text{s}^{-1}$ . The ferulate moiety is in the astaxanthin diester a better radical scavenger than free ferulic acid as seen from the rate constant of scavenging of 1-hydroxyethyl radicals in ethanol at 25°C with a second-order rate constant of  $(1.68 \pm 0.1) 10^8 \text{ L mol}^{-1}\text{s}^{-1}$  compared to  $(1.60 \pm 0.03) 10^7 \text{ L mol}^{-1}\text{s}^{-1}$  for the astaxanthin:ferulic acid mixture, 1:2 equivalents. The mutual enhancement of antioxidant activity for the newly synthesized astaxanthin diferulate becoming a bifunctional antioxidant is rationalized according to a two-dimensional classification plot for electron donation and electron acceptance capability.

© 2014 Informa UK, Ltd. This provisional PDF corresponds to the article as it appeared upon acceptance. Fully formatted PDF and full text (HTML) versions will be made available soon.

DISCLAIMER: The ideas and opinions expressed in the journal's *Just Accepted* articles do not necessarily reflect those of Informa Healthcare (the Publisher), the Editors or the journal. The Publisher does not assume any responsibility for any injury and/or damage to persons or property arising from or related to any use of the material contained in these articles. The reader is advised to check the appropriate medical literature and the product information currently provided by the manufacturer of each drug to be administered to verify the dosages, the method and duration of administration, and contraindications. It is the responsibility of the treating physician or other health care professional, relying on his or her independent experience and knowledge of the patient, to determine drug dosages and the best treatment for the patient. *Just Accepted* articles have undergone full scientific review but none of the additional editorial preparation, such as copyediting, typesetting, and proofreading, as have articles published in the traditional manner. There may, therefore, be errors in *Just Accepted* articles that will be corrected in the final print and final online version of the article. Any use of the *Just Accepted* articles is subject to the express understanding that the papers have not yet gone through the full quality control process prior to publication.

## Astaxanthin diferulate as a bifunctional antioxidant

Thiago Bueno Ruiz Papa<sup>1</sup>, Vagner Dantas Pinho<sup>1</sup>, Eduardo Sanches Pereira do Nascimento<sup>1</sup>, Willy Glen Santos<sup>1</sup>, Antonio Carlos Bender Burtoloso<sup>1</sup>, Leif Horsfelt Skibsted<sup>2</sup>, and Daniel Rodrigues Cardoso<sup>1</sup>

<sup>1</sup>Instituto de Química de São Carlos, Universidade de São Paulo, Av. Trabalhador São Carlense 400, CP 780, CEP 13560-970, São Carlos – SP, Brazil, <sup>2</sup>Department of Food Science, University of Copenhagen, Rolighedsvej 30, DK-1958 Frederiksberg C, Denmark.

**Corresponding author:** Daniel Rodrigues Cardoso, Instituto de Química de São Carlos, Universidade de São Paulo, Av. Trabalhador São Carlense 400, CP 780, CEP 13560-970, São Carlos – SP, Brazil. Tel/Fax +55 16 33 73 99 76. E-mail: [drcardoso@iqsc.usp.br](mailto:drcardoso@iqsc.usp.br)

### Abstract

Astaxanthin when esterified with ferulic acid is better singlet-oxygen quencher with  $k_2 = (1.58 \pm 0.1) 10^{10} \text{ L mol}^{-1}\text{s}^{-1}$  in ethanol at 25 °C compared to astaxanthin with  $k_2 = (1.12 \pm 0.01) 10^9 \text{ L mol}^{-1}\text{s}^{-1}$ . The ferulate moiety is in the astaxanthin diester a better radical scavenger than free ferulic acid as seen from the rate constant of scavenging of 1-hydroxyethyl radicals in ethanol at 25 °C with a second-order rate constant of  $(1.68 \pm 0.1) 10^8 \text{ L mol}^{-1}\text{s}^{-1}$  compared to  $(1.60 \pm 0.03) 10^7 \text{ L mol}^{-1}\text{s}^{-1}$  for the astaxanthin:ferulic acid mixture, 1:2 equivalents. The mutual enhancement of antioxidant activity for the newly synthesized astaxanthin diferulate becoming a bifunctional antioxidant is rationalized according to a two-dimensional classification plot for electron donation and electron acceptance capability.

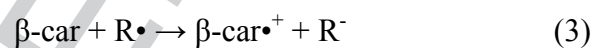
**Keywords:** carotenoid, plant phenol, antioxidant, antiradical, astaxanthin.

## Introduction

Carotenoids are important protectors of biological structures against oxidative stress both as singlet oxygen quenchers and as radical scavengers [1,2]. Singlet oxygen quenching, as is important during photosynthesis, depends on energy transfer between the electrophilic singlet oxygen and the polyene backbone of the carotenoid with rates increasing for increasing length of conjugation followed by non-radiative/radiative decay of the formed triplet-carotenoid to the ground state, eq.(1) and eq.(2) [3]:



For radical scavenging three mechanisms have now been recognized for  $\beta$ -carotene [4,5]:



electron transfer eq.(3), radical addition eq.(4) and hydrogen atom transfer eq.(5), for which the radical scavenging efficiency, as in the reaction eq.(3), depends on the electron donor capacity [6]. Keto-carotenoids like astaxanthin are poor electron donors and have, based on theoretical calculations been classified as electron acceptors in their protective functions during oxidative stress, eq.(6) [8]:



In a two dimensional donor/acceptor classification, compounds like ascorbic acid are found among the poor radical scavengers as both being a poor electron donor and a poor electron acceptor, while  $\beta$ -carotene is an example of good electron donor and at the same time good electron acceptor and accordingly a good antiradical compound. In this classification, phenolic antioxidants like the plant phenols and the tocopherols, function as good electron

donors but at the same time as poor electron acceptors, while the keto-carotenoids including astaxanthin and cantaxanthin are good electron acceptors but poor electron donors and have been termed antireductants [6,8].

It has now been recognized that antioxidant interaction may create synergism between antioxidants belonging to different groups in the donor/acceptor classification [2]. Such effects are seen at the interface between lipids and water as in membranes, where lipophilic carotenoids like  $\beta$ -carotene may protect the lipids, through radical scavenging as in the reaction of eq.(3) followed by regeneration by plant phenol, Ar-OH, eq.(7):



Such regeneration reactions have been found to be fast and important for the antioxidant synergism observed between compounds both classified as good electron acceptors as for  $\beta$ -carotene and various plant phenols but with opposite classification as electron donors [9]. Plant phenols covalently linked to carotenoid derivatives have been shown to have better function in membrane model systems with facile intermolecular electron transfer rather than electron transfer depending on bimolecular processes between the plant phenols and the carotenoid [10,11,12,13,14,15].

What remains to be studied is, however, the combination of plant phenols as good electron donors but poor electron acceptors linked covalently to a poor electron donor but good electron acceptor such as astaxanthin, Scheme 1. This double opposite combination has only been studied for bimolecular antioxidant regeneration [16]. The potential of such bifunctional molecules simultaneously functioning as antireductants and as antioxidants accordingly to the reactions of eq.(3) and eq.(6) respectively, is completely unexplored and deserves attention both in relation to singlet oxygen quenching and to radical scavenging activity.

## Materials and methods

### Chemicals

Acetonitrile, dichloromethane (DCM), dimethylformamide (DMF), ethanol (EtOH), ethyl acetate, hexane, and pyridine (Pyr) were of HPLC grade (J. T. Baker, Phillipsnurg, NJ, US). Ferric chloride (97%) and hydrogen peroxide (30%) were obtained from Merck (Darmstadt, Germany). Dichloromethane was dried over 3Å molecular sieves (Sigma-Aldrich, Steinheim, Gwermany) 24 hours prior to the experiments. Ammonium chloride (99%), cesium carbonate (Cs<sub>2</sub>CO<sub>3</sub>), 4-dimethylaminopyridine (DMAP) (99%), ferulic acid (99%), formic acid (98%), imidazole (Im) (99%), oxalyl Chloride (COCl)<sub>2</sub> (99%), α-(4-pyridyl-1-oxide)-N-tert-butyl nitron (4-POBN) (99%), tert-butyl dimethyl silyl chloride (TBDMSCl) (95%), sodium sulfate (99%), and tetrabutylammonium hexafluorophosphate were of analytical grade and purchased from Sigma-Aldrich (Steinheim, Germany). Deionized water was obtained using a Milli-Q system Millipore Co. (Billerica, MA, US).

#### Preparation of Ferulic acid TBDMS ether [17]

For the phenolic hydroxyl group with TBDMS 1.70 g (11.3 mmol) of TBDMSCl were added to a 5 mL stirred CH<sub>2</sub>Cl<sub>2</sub> 1 g (5.15 mmol) of ferulic acid, 0.77 g (11.3 mmol) of imidazole and 0.094 g (0.77 mmol) of DMAP at 0° C. The solution was returned to room temperature and the reaction was stirred until the reaction was finished. After addition of NH<sub>4</sub>Cl saturated solution, the reaction mixture was extracted three times with CH<sub>2</sub>Cl<sub>2</sub> and dried over with Na<sub>2</sub>SO<sub>4</sub>. The organic phase was concentrated and the residue purified by flash column chromatography on silica gel (ethyl acetate/hexane 2:3) to give 0.93 g (65% yields) of the desired ferulic acid TBDMS ether.

#### Preparation of Ferulic acid chloride TBDMS ether [18]

In a solution of 0.233 g (0.84 mmol) equivalent of ferulic acid TBDMS ether in 5 mL of dry CH<sub>2</sub>Cl<sub>2</sub> under Ar atmosphere, 0.16 g (1.3 mmol) of oxalyl chloride were added dropwise at 0° C. Then, 6 mg (0.084 mmol) of dry dimethylformamide (DMF) was added to the solution as catalyst. After 2 h of reaction at room temperature, the excess of oxalyl chloride was removed under reduced pressure and the solvent was removed under vacuum to yield the ferulic acid chloride TBDMS ether.

#### Synthesis of Astaxanthin diferulate

0.050 g (0.084 mmol) of astaxanthin was dissolved in 5 mL of dry CH<sub>2</sub>Cl<sub>2</sub> and 250 μL of pyridine was added under argon atmosphere. The result solution was added dropwise to a closed vial, purged with Ar, containing a solution of ferulic acid chloride TBDMS ether (0.84 mmol) in 5 mL of dry CH<sub>2</sub>Cl<sub>2</sub> at 0 °C. The reaction was kept at room temperature overnight

under stirring. The reaction solution was dissolved in  $\text{CH}_2\text{Cl}_2$  and washed with  $\text{NH}_4\text{Cl}$  saturated solution, the organic phase was dried over with  $\text{Na}_2\text{SO}_4$  and concentrated. The residue was dissolved in 10 mL of DMF/ $\text{H}_2\text{O}$  (10:1) solution and 0.274 g (0.84 mmol) of  $\text{Cs}_2\text{CO}_3$  [18] was added under stirring. After 2 h of reaction, water was added and the reaction mixture was extracted three times with ethyl acetate and dried over with  $\text{Na}_2\text{SO}_4$ , the organic phase was concentrated; the residue was diluted in  $\text{CH}_2\text{Cl}_2$  and applied to TLC plates. Purified astaxanthin diferulate were obtained after development with ethyl acetate/hexane (3:7), to give 0.063 g (yield of 80%) of astaxanthin diferulate.

#### Transient absorption laser flash photolysis

Laser flash photolysis experiments were carried out with an LFP-112 nanosecond laser flash photolysis spectrometer from Luzchem (Ottawa, Canada) using the third harmonic (355 nm) of a pulsed Quantel Nd:YAG laser (Les Ulis, France) attenuated to  $14 \text{ mJ}\cdot\text{cm}^{-2}$  as the excitation source with a 8 ns resolution. A R928 photomultiplier tube from Hamamatsu Photonics (Hamamatsu City, Japan) was used to detect the transient absorption (300-900 nm). Appropriate UV cutoff filters were used to minimize the sample degradation by the monitoring light. The samples were excited in 1.0 cm x 1.0 cm fluorescence cuvettes from Hellma GmbH. (Mulheim, Germany). Each kinetic trace was averaged 16 times and observed rate constants were determined by fitting the data with MatLab R2008. All measurements were made with fresh solutions thermostated at  $298 \pm 0.5 \text{ K}$  and purged with  $\text{N}_2$  (White-Martins, Sertãozinho-SP, Brazil) for 60 min before the experiment.

#### Singlet oxygen scavenging activity

Singlet-excited oxygen lifetime decay was recorded with a time-resolved NIR spectrofluorometer (Edinburgh Analytical Instruments, U.K.) equipped with a Nd:YAG laser (Continuum Surelite III),  $\lambda_{\text{exc}} = 532 \text{ nm}$  (4th harmonic; pulse 30 ns). The emitted light passed through silicon and an interference filter and a monochromator before detection with a NIR photomultiplier (Hamamatsu Co. R5509). The singlet oxygen lifetime was determined by

applying first-order exponential fitting to the curve of the phosphorescence decay. Methylene blue was used as singlet-excited oxygen photosensitizer in ethanol solutions at a concentration of  $1.6 \times 10^{-5} \text{ mol L}^{-1}$ . The stock solutions were made dissolving the compounds in an ethanolic solution of methylene blue ( $1.6 \times 10^{-5} \text{ mol L}^{-1}$ ), with concentrations of 1.0 g/L for the ester and astaxanthin and 3.0 g/L for ferulic acid. The singlet oxygen quenching experiments were performed by adding different aliquots of stock solutions directly to the cuvette containing methylene blue ( $1.6 \times 10^{-5} \text{ mol L}^{-1}$ ) in ethanol. A Continuum Surelite III Nd:YAG laser was used as the excitation source operating at 532 nm (5 ns, 10 Hz). The radiation emitted at 1270 nm was detected at right angles by a liquid nitrogen cooled photomultiplier from Hamamatsu R5509.

#### 1-hydroxyethyl radical scavenging activity

The formation of 1-hydroxyethyl radicals and spin trapping by 4-POBN were assayed by mixing 80  $\mu\text{L}$  of a  $\text{H}_2\text{O}_2$  solution ( $6.0 \times 10^{-2} \text{ mol L}^{-1}$ ) with the reaction mixture containing 1 mL of 4-POBN ( $3.0 \times 10^{-3} \text{ mol L}^{-1}$ ) in ethanol contain 10% (v/v) of water, 60  $\mu\text{L}$  of  $\text{FeCl}_2 \cdot 4\text{H}_2\text{O}$  ( $2.0 \times 10^{-3} \text{ mol L}^{-1}$ ), and varying concentrations of the antioxidant in oxygen free solution. The incubation time was 1 min at 25 °C, and the reaction was finally freeze-quenched in liquid nitrogen (77 K) until analysis. The competitive kinetics was conducted by monitoring the content of 1-hydroxyethyl/4-POBN by ESI-MS [20].

#### Electrochemical Studies

Cyclic voltammetry was carried out in a PAR model 264A potentiostat (Oak Ridge, TN, United States) connected to a personal computer using proprietary software for data acquisition. Electrochemical oxidations were carried out in  $\text{CH}_2\text{Cl}_2$  containing 0.1 M of tetrabutylammonium-hexafluorophosphate as the supporting electrolyte and a three-electrode system with saturated calomel, a glassy carbon or boron doped electrode for higher potential window (up to 2 V vs. NHE), and a platinum wire used as reference, work, and auxiliary electrodes, respectively.

## High-resolution accurate mass spectrometry

Direct infusion high-resolution accurate ESI-MS spectra of reaction products were performed on an LTQ-Orbitrap ESI-FT-MS model Velos from Thermo Fisher Scientific mass spectrometry system (Bremen, Germany) operating in the negative or positive ion detection mode.

## Luminescent Measurements

Fluorescence, phosphorescence and total emission were measurements were carried out using a Hitachi F-7000 fluorescence spectrometer (Hitachi High-Tech, Tokyo, Japan) at 77 K or 298 K using a quartz cold finger (Wilma-Labglass, Vineland NJ, US) or a homemade thermostated cell holder, respectively. Samples were excited in 1.0 cm × 1.0 cm fluorescence cuvettes from Hellma GmbH (Mulheim, Germany) for measurement at 298 K or using high-quality quartz EPR tubes of 4 mm i.d. (Wilma-Labglass) at 77 K. Fluorescence lifetime measurements were performed with an Optical Building Blocks Corp. Fluorometer (Birmingham, U.K.), using the fluorescence time-resolved mode. The excitation and emission wavelengths were  $\lambda = 460$  and 530 nm, respectively. Fluorescence decay times were fitted using a mono-exponential decay function and the best fit obtained by optimized Chi-square residuals and standard deviation parameters. All solutions were previously deaerated by purging the cuvette with high-purity N<sub>2</sub> (White-Martins, Sertãozinho-SP, Brazil).

## DFT calculations

In order to calculate the R<sub>d</sub> and R<sub>a</sub> indexes [7] eq.(8) and eq.(9), Density Functional Theory as implemented in Gaussian 03 [21] was employed for all calculations using the B3LYP/6-31G(d) basis set for full geometry optimization.

$$R_d = \frac{\omega_g^m}{\omega_{Na}^m} \quad (8)$$

$$R_a = \frac{\omega_g^f}{\omega_f^f} \quad (9)$$

The electrodonating power ( $\omega^-$ ) and the electroaccepting power ( $\omega^+$ ) were calculated by eq.(10) and eq.(11), respectively [22]:

$$\omega^- = \frac{(3VIE + VEA)^2}{16(VIE - VEA)} \quad (10)$$

$$\omega^+ = \frac{(VIE + 3VEA)^2}{16(VIE - VEA)} \quad (11)$$

where VIE is the vertical ionization energy and calculated as the difference between the energy of the cation and the neutral molecule, assuming that both of these have the ground-state nuclear configuration of the neutral molecule. VEA is the vertical electron affinity and calculated as the energy difference between the neutral molecule and the anion, assuming for both forms the ground-state nuclear configuration of the neutral molecule.

## Results and Discussion

Esterification of astaxanthin with ferulic acid according to the reactions of Scheme 1 gave a compound confirmed by high-resolution accurate electrospray ionization mass spectrometry and 1D and 2D  $^1\text{H}/^{13}\text{C}$  NMR to be the diester of astaxanthin, see Table 1.

The UV-visible absorption spectrum of the new compound, Figure 1, is seen to be the superimposed spectrum of the spectra of astaxanthin and the two ferulic acid building blocks indicating that the conjugation of astaxanthin was not fully enlarged to include the two ferulate esters. The new ester groups may, however, to some degree be in a keto-enol tautomeric equilibrium as shown in Scheme 1. Clearly this tautomerism, strongly shifted to the keto form, is hardly affecting the absorption spectrum, which by spectral Gaussian deconvolution could be resolved into components corresponding to astaxanthin and ferulic acid, see insert in Figure 1.

The emission spectrum of astaxanthin was in contrast strongly affected by esterification by ferulic acid, Figure 2. The fluorescence quantum yield increased by a factor of more than 10 at 77 K following excitation at 280 nm and a factor of 50 at 298 K, see Figure 2A and 2C for

fluorescent spectra and Table 2 for numerical values. The phosphorescence was likewise strongly enhanced and the quantum yield at 77 K increased from 0.03 to 0.23 for excitation at 250 nm with phosphorescence lifetime of 1.6 s for the ester compared to 0.7 s for astaxanthin, see insert in Figure 2B and 2D. The total phosphorescence of the new compound also shown in Figure 2C and 2D is remarkable intense for a carotenoid, which normally have low intersystem crossing yields to populate the triplet state [9]. The triplet state is suggested to have an increased  $\Phi_{isc}$  for the diferulated as compared to astaxanthin or that the non-radioactive deactivation is less efficient for the larger molecule.

The decay of the carotenoid triplet state was also followed using transient absorption spectroscopy, for the chloroform as electron-withdrawing solvent in order to monitor the radical cation formation from the triplet for both astaxanthin and the diferulate ester, eq.(12), see Figure 3. For chloroform, the triplet decay is marginally faster than for ethanol as solvent for both astaxanthin and the diester, which both formed the radical cation. The lifetime of the radical cation was in the ms time regime and was 20 % shorter for the diester than for astaxanthin. Notably, the transient triplet absorption spectrum (T-T) is red-shifted approximately 10 nm for the diferulate compared to astaxanthin in agreement with longer conjugation of the diester. A comparable red-shift is noted for the radical cations (D-D transition).



The reduced energy difference between the lowest triplet state and the ground state for astaxanthin diferulate as compared to astaxanthin is expected to give a better match to the singlet oxygen to ground state triplet oxygen transition in effect becoming a better singlet oxygen quencher. The second-order rate constants for quenching of  $^1\text{O}_2$  in ethanol at 25 °C obtained by time-resolved near-infrared phosphorescence spectroscopy following methylene blue formation of  $^1\text{O}_2$  were determined as shown in Figure 4 for astaxanthin, ferulic acid, and the astaxanthin diferulate and the rate constants present in Table 3. Ferulic acid does hardly

quench  $^1\text{O}_2$ , but enhance, when linked as ester, the quenching by astaxanthin by a factor of 10 as seen from the rate constant and also clearly illustrated in Figure 4. The more efficient  $^1\text{O}_2$  quenching of astaxanthin diferulate is accordingly seen to confirm the importance of lowering the carotenoid triplet state energy for facile energy transfer from  $^1\text{O}_2$ , making the ester 13-fold more reactive than free astaxanthin and greatly surpass the reactivity of lycopene ( $k_q = 3.1 \times 10^{10} \text{ L mol}^{-1} \text{ s}^{-1}$ ), the most efficient natural singlet oxygen quencher [3].

Radical scavenging of astaxanthin and astaxanthin diferulate was compared for 1-hydroxyethyl radical as a moderately reactive carbon-centered radical using a competitive kinetics approach based on 4-POBN as a spin-trap and probed by electrospray mass spectrometry [17]:



The  $\text{CH}_3(\text{CH})\text{OH-4-POBN}\bullet$  stable radical adduct was quantified and based on the known value of  $k_2$ , the value of  $k'_2$  was determined for the 3 evaluated antioxidants according:

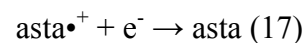
$$\frac{F}{1-F} k_2 [4\text{-POBN}] = k'_2 [\text{antioxidant}] \quad (15)$$

where F is the fraction of  $\text{CH}_3(\bullet\text{CH})\text{OH}$  trapped by 4-POBN. From the experimental values shown in Figure 5, the radical scavenging rate constant presented in Table 2 were found. Again it is seen that the radical scavenging activity of astaxanthin diferulate is enhanced by a factor of 10 compared with the 1:2 (astaxanthin:ferulic acid) antioxidant mixture.

The reaction of the astaxanthin diferulate with the 1-hydroxyethyl radical was further studied through product analysis using high resolution accurate ESI-MS. The main reaction products had the mass of 1037.55 Da, 772.43 Da, and 266.12 Da and were tentatively identified as shown in Scheme 2. From the reactions in Scheme 2, it is seen that each astaxanthin diferulate is capable of scavenging four 1-hydroxyethyl radicals and that the

radical scavenging is a radical addition centered at the ferulate moieties of the ester rather than at the polyene backbone.

The standard reduction potential for the two one-electron process related to astaxanthin, eq.(11) and eq.(12) was in CH<sub>2</sub>Cl<sub>2</sub> as solvent found to have the value of E<sub>1/2</sub> = +1.18V and +0.95V vs. NHE for asta<sup>2+</sup> and asta<sup>•+</sup> using cyclic voltammetry, respectively. For the astaxanthin diferulate the values were E<sub>1/2</sub> = +1.20V and +0.98V vs. NHE, respectively, indicating that astaxanthin diferulate is more reducing than astaxanthin. Ferulic acid in the ester had the value of E<sub>1/2</sub> = +1.58V vs. NHE compared to 1.39 V vs. NHE for the free ferulic acid. Astaxanthin accordingly makes ferulic acid less reducing and ferulic acid makes astaxanthin more reducing in the ester as compared to the precursors. The ferulate moiety is the more reducing part of the ester in agreement with addition reaction of 1-hydroxyethyl radical as shown in Scheme 2.



As seen from the estimative of the standard reduction potentials in the ester as compared to free ferulate, the electron donating capacity is reduced. Since ferulate is dominating the radical scavenging activity, of the astaxanthin diferulate, the ester is moving toward the group of good electron acceptors at the expense of electron donor capacity. The experimental verification of this change in electronic properties depends on further studies, but therefore theoretical calculations using the method described by Martinez [7] quantify the change in electronic properties in the radical scavenging activity by esterification of ferulic acid with astaxanthin, see Figure 6.

## Conclusions

Astaxanthin is becoming a better singlet oxygen scavenger through esterification with ferulic acid, at the same time, ferulic acid becomes a better radical scavenger through the

esterification. These simultaneous improvements of antioxidant activity for both the plant phenol and the carotenoid may be explained by the two dimensional electron donor/electron acceptor capacity diagram seen in Figure 6. Astaxanthin moiety is clearly modified more than ferulic acid through the esterification with respect to antioxidant properties. For organized media like cellular membranes, the esterification of carotenoids by phenolic acids may yield optimal protection through the two antioxidant function unified in the same molecule and enhance each other also with the perspective of new drug development in relation to oxidative stress in eyes and skin health.

### **Acknowledgement**

This research is part of the bilateral Brazilian/Danish Food Science Research Program “BEAM - Bread and Meat for the Future” supported by FAPESP (Grant No. 2011/51555-7 and 2009/54040) to DRC and by the Danish Research Council for Strategic Research (Grant No. 11-116064) to LHS. DRC thanks CNPq for the research fellowship. Prof. Mauricio da Silva Baptista (Chemistry Institute, University of São Paulo) is knowledge for grant the access to the time resolved NIR spectrofluorimeter.

JUST ACCEPTED

## References

- [1] Böhm F, Edge R, Truscott G. Interactions of dietary carotenoids with activated (singlet) oxygen and free radicals: Potential effects for human health *Molecular Nutrition & Food Research* 2012; 56: 205-216.
- [2] Skibsted LH. Carotenoids in antioxidant networks. Colorants or radical scavengers *Journal of Agricultural and Food Chemistry* 2012; 60: 2409-2417.
- [3] Di Mascio P, Kaiser S, Sies H. Lycopene as the most efficient biological carotenoid singlet oxygen quencher *Archives of Biochemistry and Biophysics* 1989; 274: 532-538.
- [4] Martinez A, Vargas R, Galano A. What is Important to Prevent Oxidative Stress? A Theoretical Study on Electron-Transfer Reactions between Carotenoids and Free Radicals. *Journal of Physical Chemistry B* 2009; 113: 12113-12120.
- [5] Chen, C-H, Han R-M, Liang R, Fu L-M, Wang P, Ai X-C, et al. Direct observation of the  $\beta$ -carotene reaction with hydroxyl radical. *Journal of Physical Chemistry B* 2011; 115: 2082-2089.
- [6] Martinez A. Donator-Acceptor Map and Work Function for Linear Polyene-Conjugated Molecules. A Density Functional Approximation Study. *Journal of Physical Chemistry B* 2009; 113: 3212-3217.
- [7] Martinez A.; Rodriguez-Girones MA, Barbosa A, Costas M. Donator acceptor map for carotenoids, melatonin and vitamins *Journal of Physical Chemistry A* 2008; 112: 9037-9042.
- [8] Galano A, Vargas R, Martinez A. Carotenoids can act as antioxidants by oxidizing the superoxide radical anion. *Physical Chemistry Chemical Physics* 2010; 12: 193-200.
- [9] Liang R, Chen C-H, Han R-M, Zhang J-P, Skibsted LH. Thermodynamic versus Kinetic Control of Antioxidant Synergism between beta-Carotene and (Iso)flavonoids and Their Glycosides in Liposomes. *Journal of Agricultural and Food Chemistry* 2010; 58: 9221-9227.

- [10] Zeeshan M, Sliwka H-R, Partali V, Martinez A. Electron uptake by classical electron donors: astaxanthin and carotenoid aldehydes. *Tetrahedron Letters* 2012; 53: 4522-4525.
- [11] Beutner S, Frixel S, Ernst H, Hoffmann T, Hernandez-Blanco I, Hundsdoerfer C, et al. Carotenylflavonoids, a novel group of potent, dual-functional antioxidants. *Arkivoc* 2007; 279-295.
- [12] Martin H-D, Kock S, Scherrers R, Lutter K, Wagener T, Hundsdoerfer C, et al. 3,3'-Dihydroxyisorenieratene, a Natural Carotenoid with Superior Antioxidant and Photoprotective Properties. *Angewandte Chemie-International Edition* 2009; 48: 400-403.
- [13] An C-B, Liang R, Ma X-H, Fu L-M, Zhang, J-P, Wang P, et al. Retinylisoflavonoid as novel membrane antioxidant. *Journal of Physical Chemistry B* 2010; 114: 13904-13910.
- [14] Hundsdoerfer C, Stahl W, Mueller TJJ, De Spirt S. UVA Photoprotective Properties of an Artificial Carotenylflavonoid Hybrid Molecule. *Chemical Research in Toxicology* 2012; 25: 1692-1698.
- [15] Hu F, Bu YZ, Liang R, Duan RM, Wang S, Han RM, et al. Quercetin and daidzein  $\beta$ -apo-14'-carotenoic acid esters as membrane antioxidants. *Free Radical Research* 2013; 47: 413-421.
- [16] Han R-M, Chen C-H, Tian Y-X, Zhang J-P, Skibsted LH. Fast Regeneration of Carotenoids from Radical Cations by Isoflavanoid Dianions: Importance of the Carotenoid Keto Group for Electron Transfer *Journal of Physical Chemistry A* 2010; 114: 126-132.
- [17] Fache F, Suzan N, Piva O. Total synthesis of cimracemate B and analogs. *Tetrahedron* 2005; 61: 5261-5266.
- [18] Santos S, Graca J. Glycerol  $\omega$ -hydroxyacid-ferulic acid oligomers in cork suberian structure *Holzforschung* 2006; 60: 171-177.

[19] Jiang ZY, Wang YG. A mild, efficient and selective deprotection of t-butyldimethylsilyl-protected phenols using cesium carbonate. *Tetrahedron Letters* 2003; 44: 3859-3861.

[20] de Almeida NEC; Homem-de-Mello P, De Keukeleire D, Cardoso DR. Reactivity of Beer Bitter Acids Toward the 1-Hydroxyethyl Radical as Probed by Spin-Trapping Electron Paramagnetic Resonance (EPR) and Electrospray Ionization– Tandem Mass Spectrometry (ESI– MS/MS). *Journal of Agricultural and Food Chemistry* 2011; 59: 4183-4191.

[21] Frisch MJ, Trucks GW, Schlegel HB, Scuseria GE, Robb MA, Cheeseman JR, et al. *Gaussian 03*; Gaussian, Inc: Wallingford, CT, 2004.

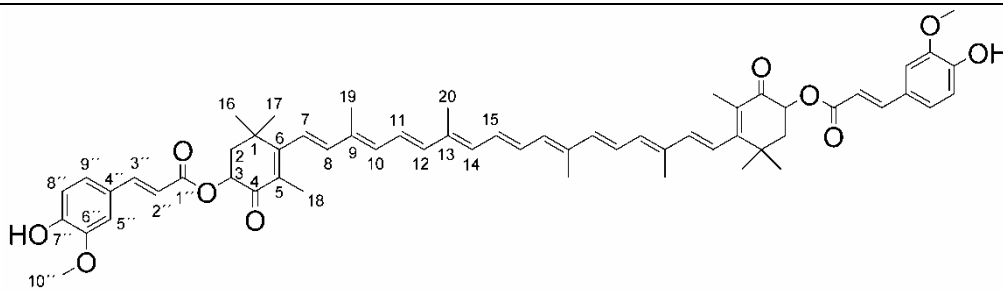
[22] Gazquez JL, Cedillo A, Vela A. Electrodonating and electroaccepting powers. *Journal of Physical Chemistry A* 2007; 111: 1966-1970.

JUST ACCEPTED

## Table Legends

**Table 1.** NMR data collected for astaxanthin diferulate in DMSO-*d*<sub>6</sub> at 25 °C.

Position	<sup>13</sup> C ( )	<sup>1</sup> H , multiplet, ( <i>J</i> in Hz)	COSY	HSQC	HMBC
1, 1'	36.7	-	-	C <sub>1,1'</sub>	-
2, 2' <sub>eq</sub> 2, 2' <sub>ax</sub>	42.1	2.04-2.14 m	H <sub>3,3'</sub>	C <sub>2,2'</sub>	C <sub>1,1'</sub> , C <sub>3,3'</sub> , C <sub>4,4'</sub> , C <sub>6,6'</sub> , C <sub>16,16'</sub>
3, 3'	70.4	5.56 dd (12.9; 6.3)	H <sub>2,2'</sub>	C <sub>3,3'</sub>	C <sub>1,1'</sub> , C <sub>2,2'</sub> , C <sub>1'',1'''</sub> , C <sub>4,4'</sub>
4, 4'	193.6	-	-	C <sub>4,4'</sub>	-
5, 5'	127.0	-	-	C <sub>5,5'</sub>	-
6, 6'	160.5	-	-	C <sub>6,6'</sub>	-
7, 7'	123.4	6.32 d (16.3)	H <sub>8,8'</sub>	C <sub>7,7'</sub>	C <sub>1,1'</sub> , C <sub>5,5'</sub> , C <sub>8,8'</sub> , C <sub>9,9'</sub> , C <sub>10,10'</sub>
8, 8'	141.8	6.57 d (16.3)	H <sub>7,7'</sub>	C <sub>8,8'</sub>	C <sub>6,6'</sub> , C <sub>9,9'</sub> , C <sub>10,10'</sub> , C <sub>19,19'</sub>
9, 9'	135.0	-	-	C <sub>9,9'</sub>	-
10, 10'	134.8	6.46 d (11.8)	H <sub>11,11'</sub>	C <sub>10,10'</sub>	C <sub>8,8'</sub> , C <sub>12,12'</sub> , C <sub>19,19'</sub>
11, 11'	125.0	6.67-6.83 m	H <sub>10, 10'; H<sub>12,12'</sub></sub>	C <sub>11,11'</sub>	C <sub>9,9'</sub> , C <sub>10,10'</sub> , C <sub>13,13'</sub>
12, 12'	139.3	6.51 d (14.8)	H <sub>11,11'</sub>	C <sub>12,12'</sub>	C <sub>9,9'</sub> , C <sub>10,10'</sub> , C <sub>13,13'</sub> , C <sub>14,14'</sub> , C <sub>20,20'</sub>
13, 13'	136.5	-	-	C <sub>13,13'</sub>	-
14, 14'	133.7	6.39-6.43 m	H <sub>15,15'</sub>	C <sub>14,14'</sub>	C <sub>15,15'</sub>
15, 15'	130.9	6.76-6.83 m	H <sub>14,14'</sub>	C <sub>15,15'</sub>	C <sub>13,13'</sub> , C <sub>14,14'</sub>
16, 16'	25.8	1.37 s	-	C <sub>16,16'</sub>	C <sub>1,1'</sub> , C <sub>2,2'</sub> , C <sub>6,6'</sub> , C <sub>17,17'</sub>
17, 17'	29.9	1.22 s	-	C <sub>17,17'</sub>	C <sub>1,1'</sub> , C <sub>2,2'</sub> , C <sub>3,3'</sub> , C <sub>6,6'</sub> , C <sub>16,16'</sub>
18, 18'	13.8	1.83 s	-	C <sub>18,18'</sub>	C <sub>4,4'</sub> , C <sub>5,5'</sub> , C <sub>6,6'</sub> , C <sub>8,8'</sub> , C <sub>16,16'</sub>
19, 19'	12.2	2.01 s	-	C <sub>19,19'</sub>	C <sub>8,8'</sub> , C <sub>9,9'</sub> , C <sub>10,10'</sub>
20, 20'	12.5	1.97 s	-	C <sub>20,20'</sub>	C <sub>12,12'</sub> , C <sub>13,13'</sub> , C <sub>14,14'</sub>
1'', 1'''	165.7	-	-	C <sub>1'',1'''</sub>	-
2'', 2'''	114.0	6.57 d (15.8)	H <sub>3'',3'''</sub>	C <sub>2'',2'''</sub>	C <sub>3,3'</sub> , C <sub>1'',1'''</sub> , C <sub>4'',4'''</sub> , C <sub>5'',5'''</sub>
3'', 3'''	145.6	7.60 d (15.8)	H <sub>2'',2'''</sub>	C <sub>3'',3'''</sub>	C <sub>1'',1'''</sub> , C <sub>2'',2'''</sub> , C <sub>4'',4'''</sub> , C <sub>5'',5'''</sub> , C <sub>6'',6'''</sub> , C <sub>9'',9'''</sub>
4'', 4'''	125.4	-	-	C <sub>4'',4'''</sub>	-
5'', 5'''	111.1	7.36 s	-	C <sub>5'',5'''</sub>	C <sub>3'',3'''</sub> , C <sub>7'',7'''</sub> , C <sub>9'',9'''</sub>
6'', 6'''	147.9	-	-	C <sub>6'',6'''</sub>	-
7'', 7'''	149.4	-	-	C <sub>7'',7'''</sub>	-
8'', 8'''	115.4	6.80 d (8.2)	H <sub>9'',9'''</sub>	C <sub>8'',8'''</sub>	C <sub>5'',5'''</sub> , C <sub>4'',4'''</sub> , C <sub>6'',6'''</sub> , C <sub>7'',7'''</sub>
9'', 9'''	123.2	7.14 d (8.2)	H <sub>8'',8'''</sub>	C <sub>9'',9'''</sub>	C <sub>3'',3'''</sub> , C <sub>5'',5'''</sub>
10'', 10'''	55.6	3.83 s	-	C <sub>10'', 10'''</sub>	C <sub>5'',5'''</sub> , C <sub>6'',6'''</sub>
7'', 7'''- OH	-	9.63 brs	-	-	-



Orbitrap FT-MS ESI<sup>+</sup>: calculated for C<sub>60</sub>H<sub>69</sub>O<sub>10</sub> 949.48907; found 949.49261 error of 4.3 ppm

JUST ACCEPTED

**Table 2.** Photophysical properties of ferulic acid, astaxanthin and astaxanthin diferulate in ethanol.

Photophysical properties	Compounds		
	ferulic acid	astaxanthin	astaxanthin diferulate
abs (nm)	230, 289, 318	226, 290, 316, 345, 478	240, 294, 329, 345, 478
F (nm)	290, 390	285, 310, 360	322, 334, 347
$\epsilon$ ( $M^{-1} cm^{-1}$ )	22,000 (318 nm)	125,000 (472 nm)	95,800 (486 nm); 54,600 (329 nm)
$F_{exc=250}$ (nm)	0.010 (77 K); 0.002 (298 K)	0.015 (77 K); 0.004 (298 K)	0.190 (77 K); 0.180 (298 K)
$P_{(77K)}$	0.001	0.003	0.230
$P_{(77K)}$	–	0.7 s	1.6 s
$\lambda_{max}(T-T)$	–	450 nm	440 nm
$T$	–	5.2 $\mu s$	4.1 $\mu s$
$\lambda_{max}(\text{radical})$	–	860 nm	850 nm
$\tau(\text{radical})$	–	2.4 ms	2 ms
$E_{S1}$	3.46 eV	4.33 eV	4.16 eV
$E_{T1}$	3.35 eV	3.87 eV	3.54 eV

abs= absorption wavelength,  $F$  = fluorescence emission wavelength,  $\epsilon$  = molar extinction coefficient,  $F$  = fluorescence quantum yield,  $exc$  = excitation wavelength,  $P$  = phosphorescence quantum yield,  $P$  = phosphorescence lifetime,  $\lambda_{max}(T-T)$  = **maximum absorption wavelength for the triplet-triplet transition**  $T$  = **triplet state lifetime**,  $\lambda_{max}(\text{radical})$  = **maximum absorption wavelength for the doublet-doublet transition**,  $\tau(\text{radical})$  = radical lifetime,  $E_{S1}$  = **singlet excited state energy**,  $E_{T1}$  = **triplet excited state energy**

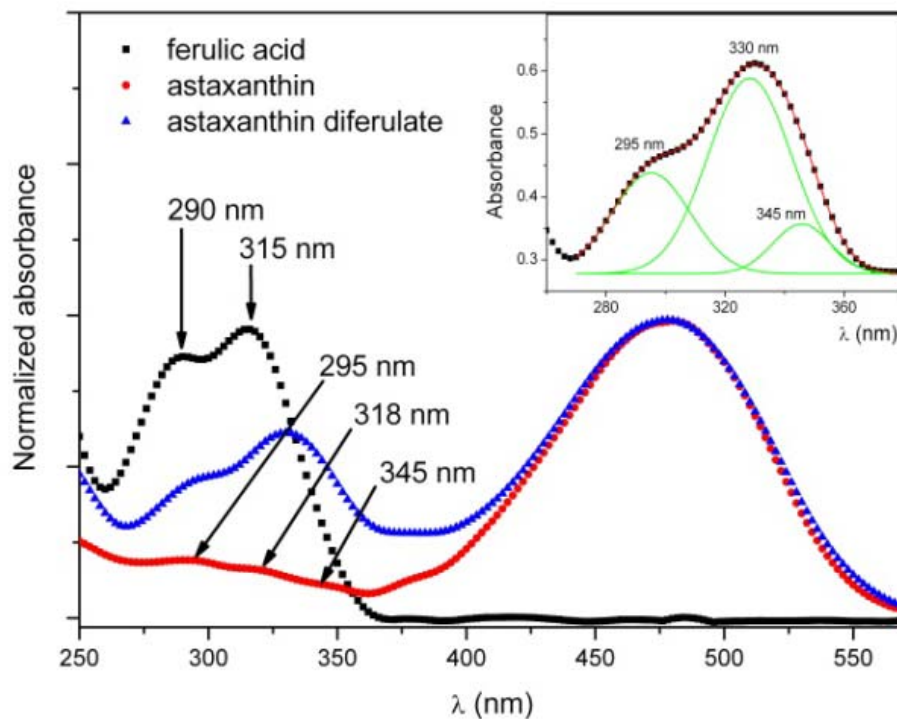
**Table 3.** Second-order rate constants for 1-hydroxyethyl radical scavenging and singlet-excited oxygen deactivation by selected antioxidants and mixture at  $25 \pm 0.1$  °C in ethanol solutions.

Antioxidant	1-hydroxyethyl radical $k_2 / (10^8 \text{ L mol}^{-1} \text{ s}^{-1})$	$^1\text{O}_2$ $k_q / (10^{10} \text{ L mol}^{-1} \text{ s}^{-1})$
astaxanthin diferulate	$1.68 \pm 0.10$	$1.58 \pm 0.10$
astaxanthin	$0.18 \pm 0.02$	$0.12 \pm 0.01$
ferulic acid	$0.02 \pm 0.01$	not observed
astaxanthin:ferulic acid (1:2)	$0.16 \pm 0.03$	-

JUST ACCEPTED

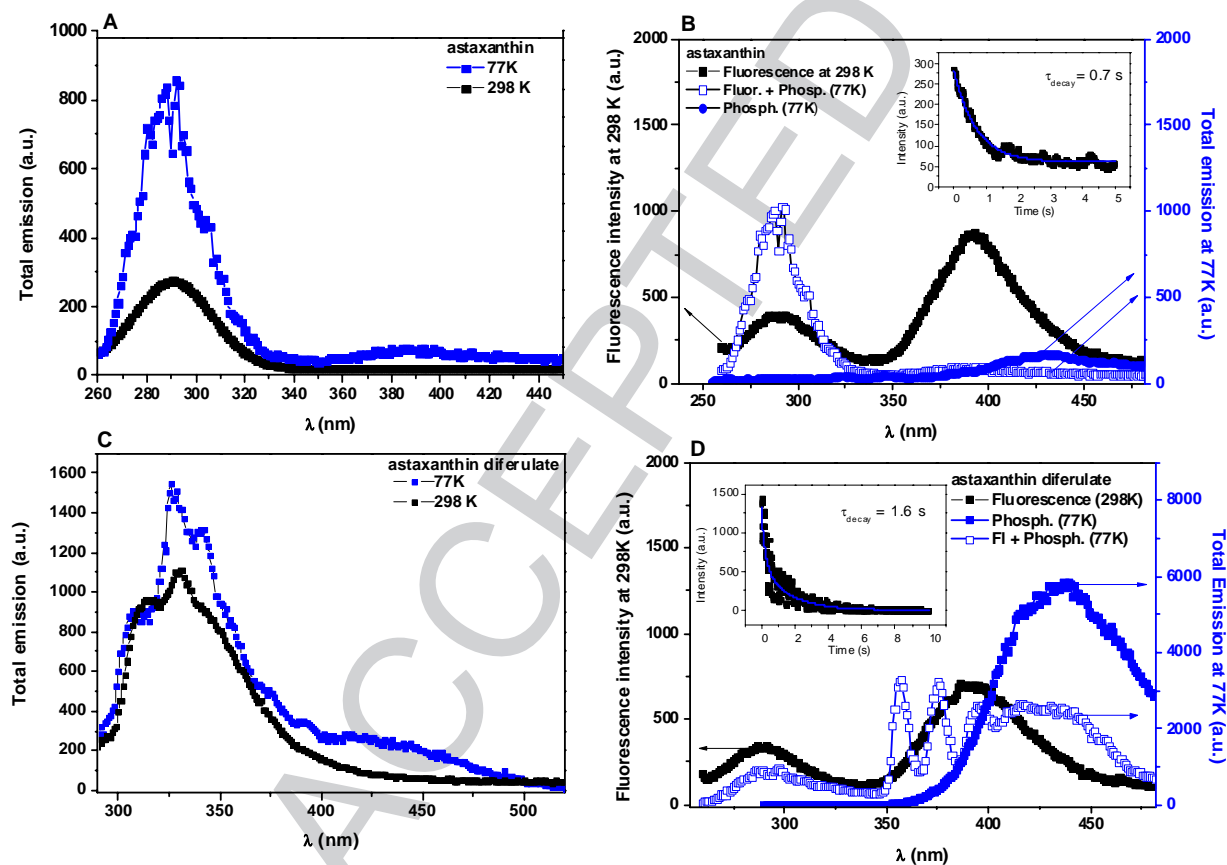
## Figure Legends

**Figure 1.** Normalized absorbance spectra of astaxanthin, ferulic acid and astaxanthin diferulate in ethanol at room temperature. Absorbance normalized for ferulic acid at maximum 320 nm and for astaxanthin and astaxanthin diferulate at 472 nm. Insert: UV band of astaxanthin diferulate resolved into components using spectral Gaussian deconvolution.



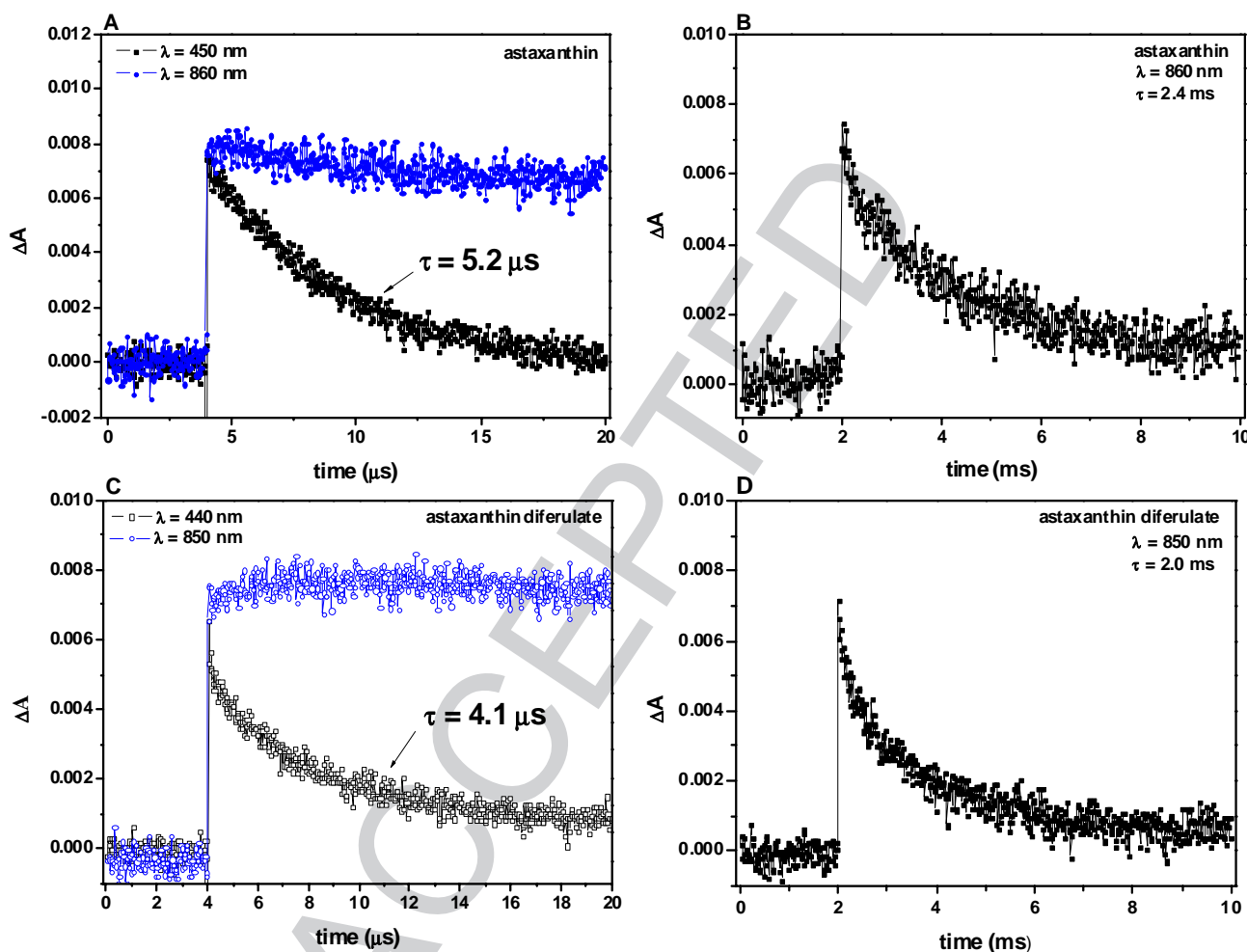
JUSTAC

**Figure 2.** Luminescence spectrum of astaxanthin and astaxanthin diferulate in ethanol at 77 K and 298 K. A) Total emission of astaxanthin at 298 K and 77 K in ethanol. B) Fluorescence and phosphorescence spectra of astaxanthin, inset display the time trace for the phosphorescence decay at 77 K in ethanol. C) Total emission of astaxanthin diferulate at 298 K and 77 K in ethanol. D) Fluorescence and phosphorescence spectra of astaxanthin diferulate, inset display the time trace for the phosphorescence decay at 77 K in ethanol. Arrows indicate the corresponding y-axis (fluorescence intensity at 298K or total emission at 77K) for the plotted spectra.



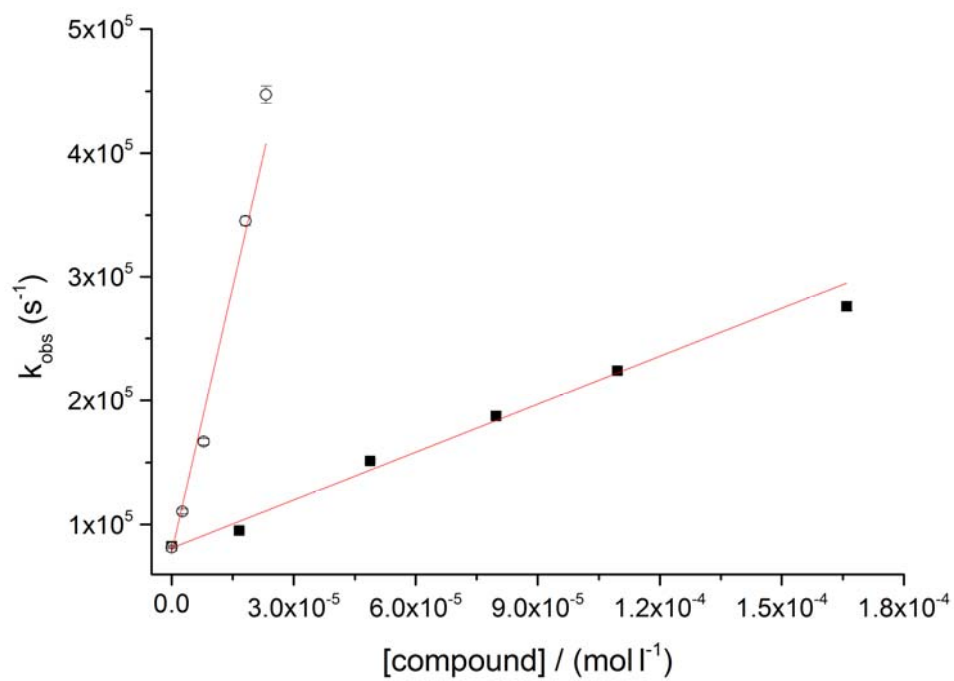
JUST

**Figure 3.** Transient difference absorbance decay observed at different wavelengths upon excitation with 8 ns laser pulses ( $14 \text{ mJ cm}^{-2}$ ) at 355 nm of Ar saturated  $\text{CH}_2\text{Cl}_2$  solutions of  $1.0 \times 10^{-6} \text{ mol L}^{-1}$  astaxanthin (upper panels) and  $1.0 \times 10^{-6} \text{ mol L}^{-1}$  astaxanthin diferulate (lower panels). Each trace is the average of 16 independent decays at  $25^\circ\text{C}$ .



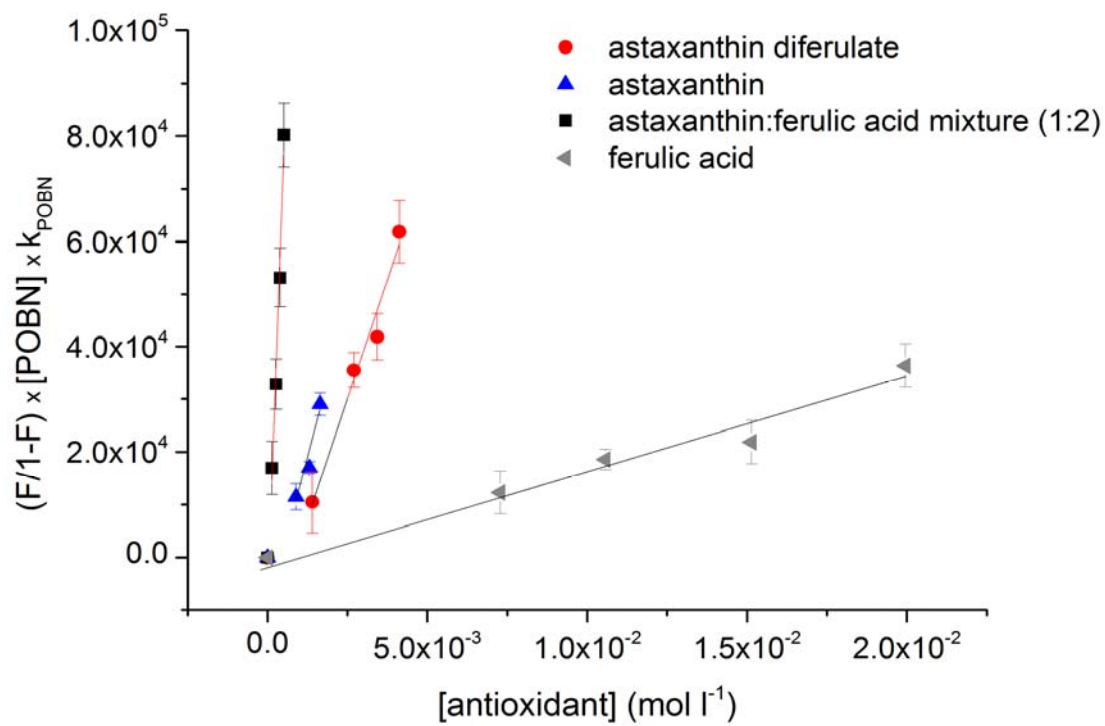
JUST A  
RIGHTS LINK

**Figure 4.** Plot of experimentally determined rate observed rate constant ( $k_{\text{obs}}$ ) for singlet oxygen as function of the antioxidant concentration. Second-order rate constant for singlet-excited oxygen deactivation is obtained from the slope of the linear regression.



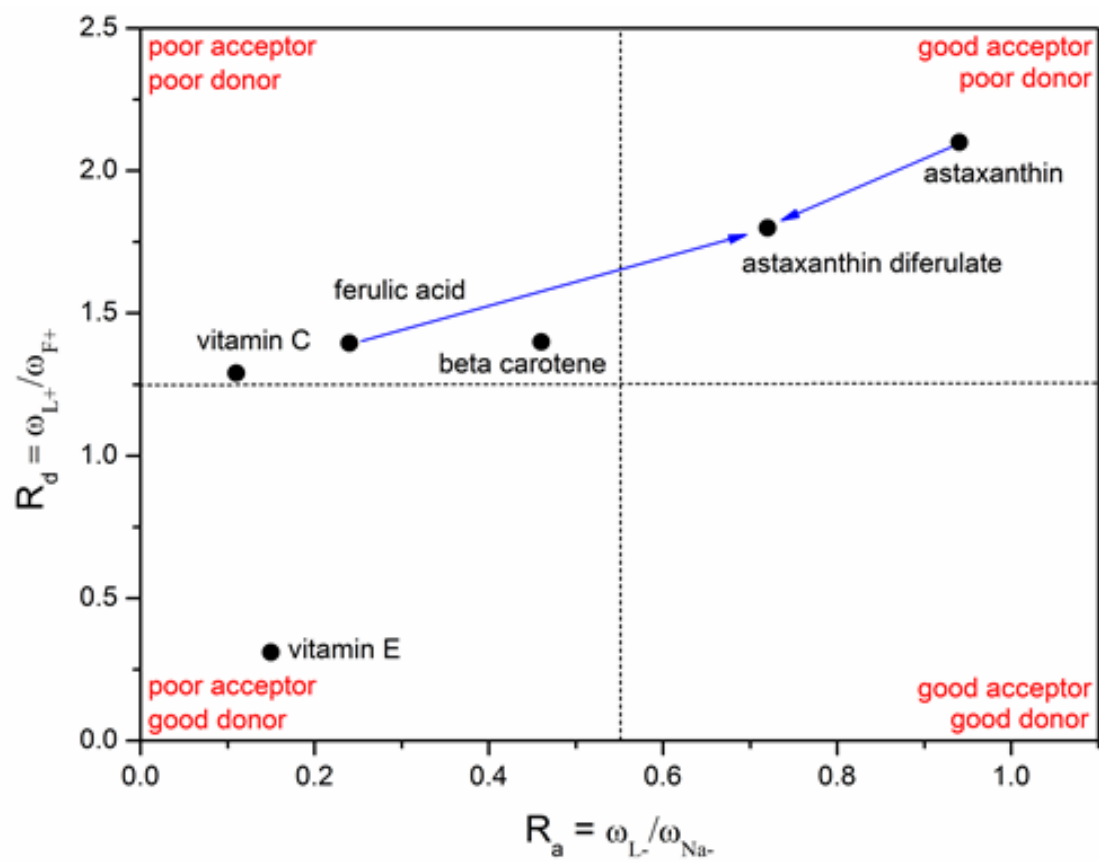
JUST ACCE

**Figure 5.** Plot of  $\frac{F}{1-F} \times k_1 \times [4-POBN]$  vs. the antioxidant concentration as obtained by spin-trapping ESI-MS.



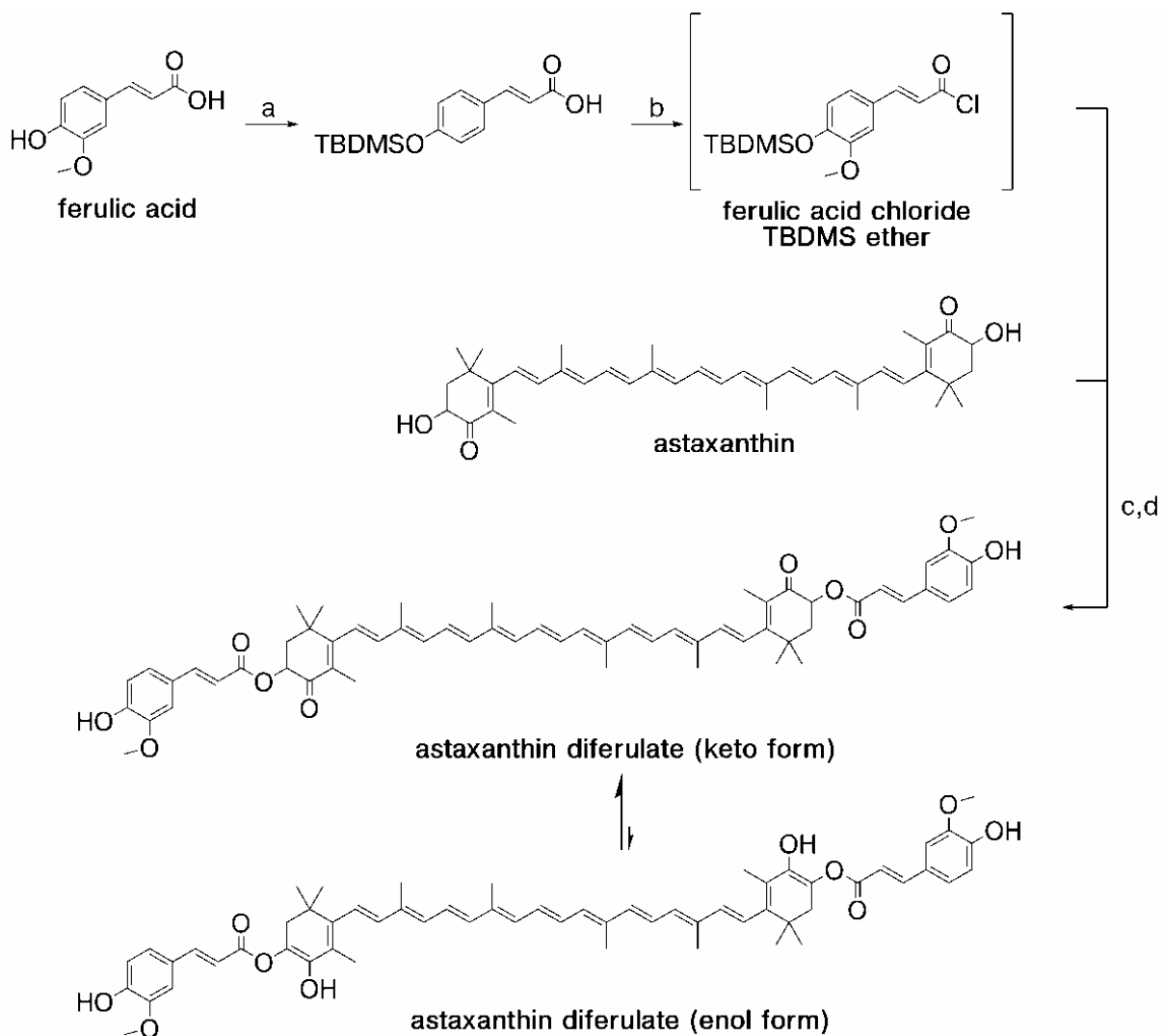
JUST ACCEPT

**Figure 6.** Donator-acceptor map for selected antioxidants including the astaxanthin diferulate and its precursors based on the theoretically calculated electrodonating ( $\omega^-$ ) and eletroaccepting ( $\omega^+$ ) power in relation to Na and F respectively [6].



JUSTAC

**Scheme 1.** Synthesis of astaxanthin diferulate. Reagents and conditions: (a) Im, DMAP, TBDMSCl, DCM; (b) (COCl)<sub>2</sub>, DMF(cat); (c) Pyr, DCM and (d) Cs<sub>2</sub>CO<sub>3</sub>, DMF:H<sub>2</sub>O (1:10).



JUST

**Scheme 2.** Proposed reaction mechanism for 1-hydroxyethyl radical scavenging by astaxanthin diferulate based on high resolution accurate ESI-MS data.

